Delivery Platforms

DOI: 10.1002/anie.201104514

Oligonucleotide Delivery by Cell-Penetrating "Striped" Nanoparticles**

Christopher M. Jewell, Jin-Mi Jung, Prabhani U. Atukorale, Randy P. Carney, Francesco Stellacci, and Darrell J. Irvine**

Gold nanoparticles (AuNPs) hold great interest in drug delivery because these materials can be functionalized with a range of biological cargos, induce minimal toxicity, and can be efficiently cleared from the body.[1] For example, many studies have described conjugation of DNA or RNA to particle surfaces in well-defined configurations, and these materials have been applied in numerous biological and therapeutic settings.[1,2] Devising new ways to mediate cell entry by AuNPs is a central area of interest.

When mixed self-assembled monolayers of dislike molecules are used to coat AuNPs, nanoscale domains spontaneously form in the particles' ligand shell. In particular, "stripe-like" domains form for ca. 1:1 binary mixed ligand compositions.[3] The formation of these domains provides AuNPs with structure-dependent properties.[4] We recently reported the unexpected finding that highly water-soluble "striped" NPs coated with sulfonate- and methyl-terminated ligands are capable of penetrating the plasma membrane of cells through non-endocytic energy-independent mechanisms, in contrast to AuNPs bearing similar ligands in random configurations, which are only endocytosed.[2b,3c,5] Given our finding that membrane penetration is highly sensitive to ligand arrangement, a major question raised by this study was whether the membrane penetration mechanism would support the transport of AuNP-conjugated drug cargos into cells, especially large, membrane-impermeable hydrophilic macromolecules that are the most challenging agents for drug delivery. Here we report on the cellular uptake of striped NPs (and non-striped control NPs) conjugated with thiol-terminated DNA oligonucleotides (ODNs), in order to answer this fundamental question and determine how cell entry of striped particles is influenced by cargo size and structure.

To quantify the extent to which AuNPs enter cells, we used BODIPY fluorescent dye to label NPs with either of two ligand compositions selected from our past work:[5] 11-mercapto-1-undecanesulphonate (MUS) alone, or a mixed shell of MUS and 1-octanethiol (MUS-OT). These particles had a core diameter of 4.6 ± 1.5 nm (Supporting Information, Figure S1), in agreement with our past findings.[5,6] Our recent work with photothermal imaging of AuNPs confirms the validity of fluorescence studies despite the small quenching effect mediated by the particle core.[7] In our past studies, we showed that striped MUS-OT NPs were capable of cell membrane penetration in dendritic cells and fibroblast cell lines, while non-striped MUS NPs were internalized by endocytic/pinocytic pathways.[5] With potential therapeutic applications for cancer in mind, we tested whether similar particle uptake would be obtained with tumor cells. B16-F0 melanoma cells were incubated with fluorescent MUS or MUS-OT NPs in serum-free medium at 37 °C for 4 h, and cellular uptake was assessed by flow cytometry. Quantitative analysis revealed significantly different uptake of each AuNP type (Figure 1 a–c; $p < 0.001$), with MUS NPs entering 51 ± 4.3 % of cells and MUS-OT NPs entering nearly all cells (96 ± 0.3 %). In agreement with our past microscopy studies, under conditions that inhibited endocytosis (4 °C), the ability of MUS NPs to enter cells was almost completely abolished (4.4 ± 0.5 %), while MUS-OT NPs still entered a significant fraction of tumor cells (32 ± 4.8 %; Figure 1 a,c; $p < 0.01$). Notably, AuNP uptake was not associated with acute toxicity (i.e., cells remained $DAPI^{low}$, Figure 1 a). These results confirm quantitatively that striped AuNPs can be taken up by tumor cells through endocytosis-independent pathways.

To test whether striped NPs retain their remarkable cell entry properties when linked to non-membrane-permeable macromolecules, we conjugated fluorophore-tagged short (12 base pair (BP)) thiolated ODN sequences of double-stranded DNA (dsDNA) to MUS or MUS-OT AuNPs via a place exchange reaction (Scheme 1).[5,8] The number of ODN molecules conjugated to AuNPs was measured by DNA displacement (see Supporting Information),[9] and after removal of unbound DNA, the dsDNA conjugated to AuNP surfaces determined by fluorescence was 2.1 ± 0.2 dsDNA molecules/AuNP (Figure S2). Since as few as 35 oligonucleotide molecules/cell can exert sustained biological effects,[10] we expect this level of conjugation to be sufficient for achieving therapeutic outcomes in future studies.

[*] Dr. C. M. Jewell,[+] Dr. J.-M. Jung,[+] P. U. Atukorale, Prof. D. J. Irvine
Depts. of Materials Science and Engineering and Biological Engineering, Koch Institute for Integrative Cancer Research
Ragon Institute of MGH, MIT, and Harvard
Massachusetts Institute of Technology, Cambridge, MA 02139 (USA)
E-mail: djirvine@mit.edu
Prof. D. J. Irvine
Howard Hughes Medical Institute, Chevy Chase, MD 20815 (USA)
R. P. Carney, Prof. F. Stellacci
Institute of Materials
École Polytechnique Fédérale de Lausanne (EPFL)
1015 Lausanne (Switzerland)
E-mail: francesco.stellacci@epfl.ch
[+] These authors contributed equally to this work.

[**] C.M.J. is supported by a postdoctoral fellowship from the Ragon Institute. J.M. is supported by the Korea Research Foundation Grant (KRF-2008-357-D00090). D.J.I. is an investigator of the Howard Hughes Medical Institute.

Supporting information for this article is available on the WWW under http://dx.doi.org/10.1002/anie.201104514.

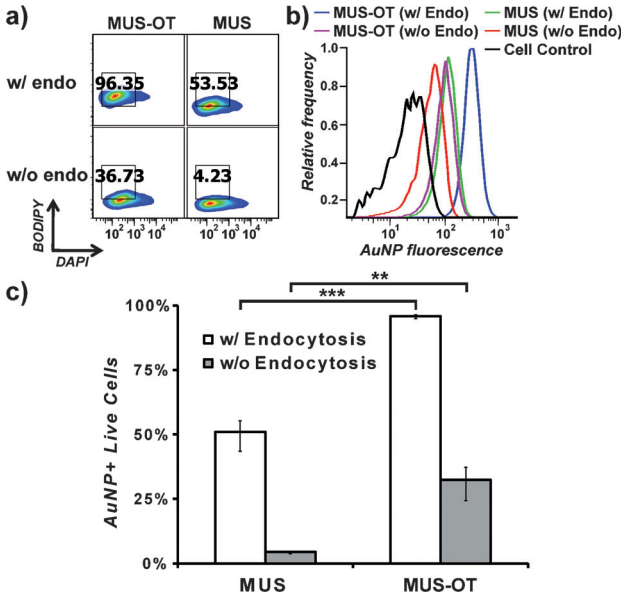

Figure 1. AuNPs with "striped" ligand shells (MUS-OT) mediate increased cell entry compared with AuNPs with homogeneous ligand shells (MUS) in the presence or absence of endocytosis. a) Flow cytometry scatter plots demonstrating the frequency of live ($DAPI^{low}$) B16-F0 cells positive for fluorescent AuNPs. b) Histograms of cell uptake of AuNPs for each ligand structure. c) Comparison of tumor cell uptake of MUS and MUS-OT AuNPs (**, $p<0.01$; ***, $p<0.001$).

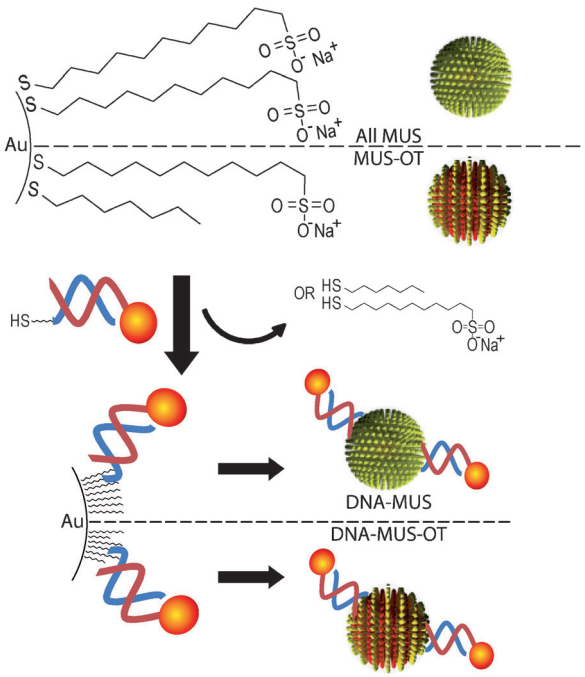

Scheme 1. Synthesis of DNA-conjugated AuNPs with homogeneous or ordered "striped" surface ligand structures. A place-exchange reaction was used to conjugate thiol-terminated fluorescent ODNs to MUS or MUS-OT ligand shells, expelling MUS or MUS-OT ligands from either AuNP type.

Using flow cytometry to measure cellular uptake, AuNPs functionalized with fluorophore-conjugated dsDNA were incubated with B16-F0 cells. As shown in Figure 2a,b, uptake of free DNA (i.e., unconjugated) by tumor cells was minimal after 4 h, while uptake patterns of MUS- or MUS-OT-conjugated ODNs mirrored earlier results seen with NPs alone. In comparing the uptake of MUS-OT AuNPs conjugated with either BODIPY (Figure 1a, 96%) or ODNs (Figure 2a, 59%), a decrease of ≈35% is observed. One explanation for this decrease could be the establishment of a steric barrier that partially inhibits cell penetration when MUS-OT particles are conjugated to ODNs. These macromolecules might partly mask ligand shell effects since the oligos have sizes comparable to or larger than AuNPs themselves. However, as seen later in Figure 2c, the modest decrease observed does not prevent substantial amounts of oligo uptake into cells.

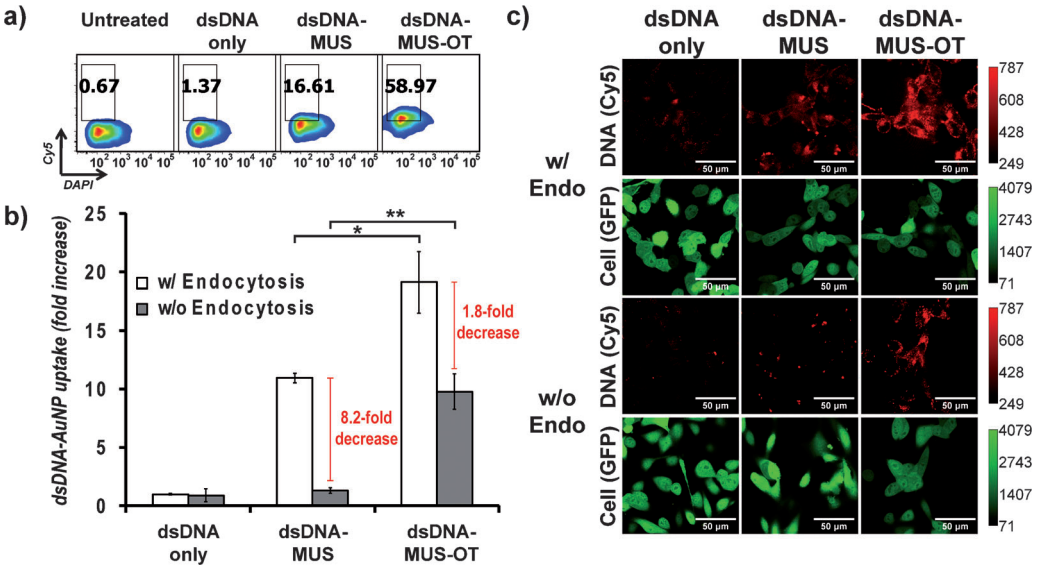

Figure 2. Ligand functionalized AuNPs mediate efficient dsDNA delivery to cells through ligand stucture-dependent entry mechanisms. B16-F0 melanoma cells were incubated for 4 h in serum-free medium with free Cy5-labeled dsDNA or Cy5-DNA-functionalized AuNPs. a) Flow cytometry histograms demonstrating uptake of DNA and cell viability (DAPI) under normal cell culture conditions. b) Relative frequency of $dsDNA^{+}$ cells (normalized to frequency of cells taking up free dsDNA under endocytic conditions), assessed by flow cytometry in the presence (white bars) or absence (grey bars) of endocytosis (*, $p<0.05$; **, $p<0.01$). c) CLSM analysis of AuNP-mediated delivery of fluorescent DNA (red channel) to B16-F0 melanoma cells expressing green fluorescent protein (GFP, green channel) as a cytosolic/nuclear marker.

Next endocytosis was blocked with pharmacological inhibitors, and uptake was reduced, but strikingly, substantial amounts of DNA-striped NP conjugates (MUS-OT) still entered cells, while DNA-MUS-NPs did not (Figure 2b). DNA-NP internalization was non-toxic as indicated by negligible increases in the population of non-viable cells (i.e., $DAPI^+$) for both MUS and MUS-OT NPs. This observation is in contrast to many lipid and polymer ODN carriers, where significant cytotoxicity is associated with cargo uptake. Similar experiments evaluating DNA-NP uptake by confocal laser scanning microscopy (CLSM) confirmed the findings in Figure 2a,b, with low to moderate levels of DNA uptake obtained with MUS AuNPs, and high levels observed with MUS-OT AuNPs under normal (i.e., endocytic) culture conditions (Figure 2c, top). As in past studies with cargo-free striped MUS-OT NPs,[5] ODNs accumulated in the cytosol but not the nucleus of cells. With active endocytic processes blocked, we observed near-baseline levels of uptake with MUS AuNPs (Figure 2c, bottom), and these punctate structures were located mainly on cell peripheries, suggesting association of NPs with cells, but lack of uptake (Figure S3). In contrast, DNA delivery mediated by MUS-OT NPs persisted in the absence of endocytosis (Figure 2c, bottom). Together, these findings indicate that striped NPs retain endocytosis-independent cell penetration properties when conjugated to DNA ODNs, promoting enhanced uptake compared to hydrophilic MUS NPs.

To determine the range of ODN lengths and types that can be delivered using ligand-ordered NPs, we prepared MUS and MUS-OT NPs conjugated with single stranded (ss) or ds DNA 12–50 BPs in length. Incubation of NPs with B16-F0 cells for 4 hr revealed that both MUS and MUS-OT NPs mediate ODN uptake across all tested oligo lengths (Figure 3). In each case, we observed the highest DNA delivery levels with MUS-OT NPs (Figure 3a). Unexpectedly, dsDNA cell entry did not change significantly as length increased (Figure 3a,b). However for ssDNA, cell entry decreased with increasing ODN length for both MUS and MUS-OT NPs (Figure 3a,c). While a mechanistic study of this effect is ongoing, dsDNA is more rigid than ssDNA, and this is known to impact DNA compaction.[11] We speculate this difference in rigidity may lead to different steric hindrance upon conjugation of ssDNA or dsDNA to AuNPs, masking the stripe-like domains that confer membrane penetration.

We have demonstrated that AuNPs coated with stripe-like self-assembled domains can deliver a range of lengths and types of DNA cargo to cells without observable toxicity. Importantly, the mechanisms by which these materials mediate entry is dependent on specific ordering of the ligand shell, with homogeneous MUS ligand structures achieving DNA delivery through endocytic pathways, and "striped" MUS-OT NPs mediating delivery though both endocytosis and cell penetration. Follow-on studies exploiting this platform in a therapeutic capacity will need to address several important questions including the choice of functional payload (e.g., immunostimulatory DNA, siRNA, miRNA, antisense delivery) and characterization of cargo release kinetics (or demonstration of bioactivity of particle-bound oligos). Oligo stability and targeting are also critical parameters, though numerous past studies have demonstrated that surface-conjugated oligos can mediate bioactivity in vitro and in vivo.[12] Targeting of cargo-loaded AuNPs to specific cells or tissues (e.g., tumors) might be achieved by several strategies, such as delivering siRNA targeting tumor-specific genes to eliminate effects on non-tumor tissues that are penetrated by AuNPs. Another targeting strategy is reversible masking of particles by conjugation of cleavable PEG molecules or targeting agents to AuNPs, temporarily disabling cell pene-

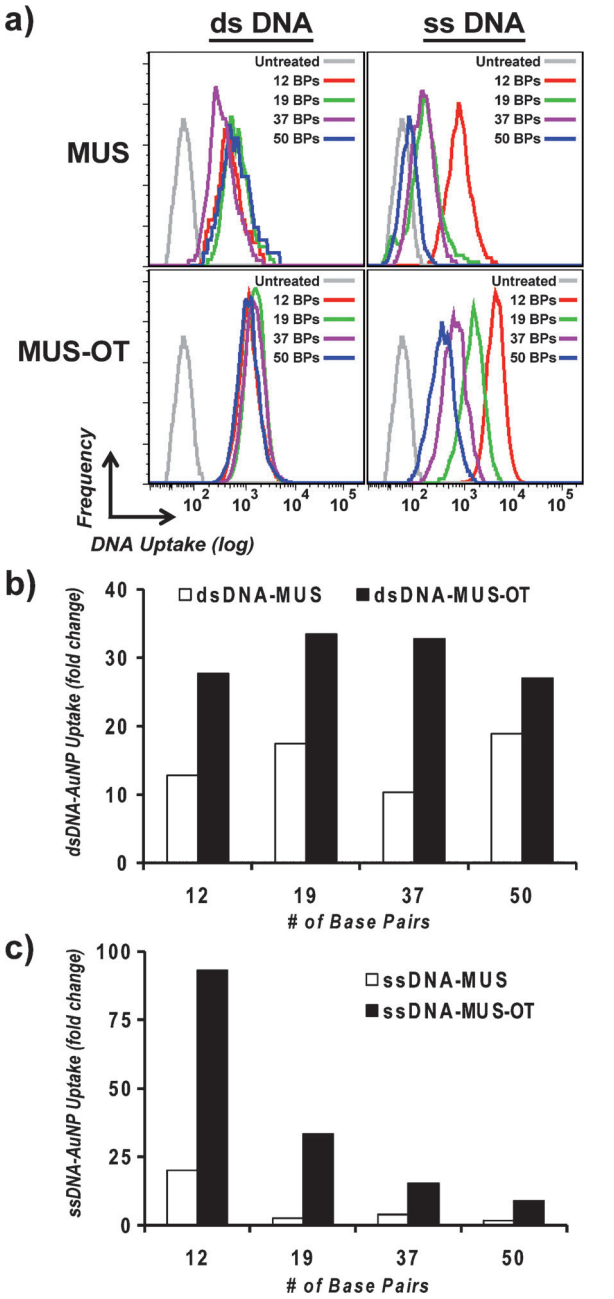

Figure 3. Delivery of fluorescent ss or ds DNA ODNs of varying length by MUS or MUS-OT AuNPs. a) Flow cytometry histograms of DNA entry mediated by NPs conjugated with ODNs of 12–50 BPs. b) and c) Relative increase in mean fluorescence intensity of cells treated with AuNPs functionalized with b) dsDNA or c) ssDNA compared to control untreated cells.

trating activity until particles accumulate in target tissue or tumor sites (e.g., by the EPR effect). The striped NP platform is readily amenable to such approaches,[13] and this second route could also provide increased cargo stability. These questions are active research areas that build on the robust cell-penetrating activity observed in this initial report, and could ultimately lead to new preventative or therapeutic strategies that bypass endocytic delivery barriers using striped AuNPs.

Received: June 30, 2011
Revised: August 17, 2011
Published online: October 26, 2011

Keywords: DNA delivery · endocytosis · gene therapy · gold nanoparticles · ligands (organic)

[1] a) E. Boisselier, D. Astruc, *Chem. Soc. Rev.* **2009**, *38*, 1759 – 1782; b) B. Duncan, C. Kim, V. M. Rotello, *J. Controlled Release* **2010**, *148*, 122 – 127; c) D. A. Giljohann, D. S. Seferos, W. L. Daniel, M. D. Massich, P. C. Patel, C. A. Mirkin, *Angew. Chem.* **2010**, *122*, 3352 – 3366; *Angew. Chem. Int. Ed.* **2010**, *49*, 3280 – 3294.

[2] a) N. L. Rosi, D. A. Giljohann, C. S. Thaxton, A. K. Lytton-Jean, M. S. Han, C. A. Mirkin, *Science* **2006**, *312*, 1027 – 1030; b) A. Verma, F. Stellacci, *Small* **2010**, *6*, 12 – 21.

[3] a) A. M. Jackson, J. W. Myerson, F. Stellacci, *Nat. Mater.* **2004**, *3*, 330 – 336; b) A. M. Jackson, Y. Hu, P. J. Silva, F. Stellacci, *J. Am. Chem. Soc.* **2006**, *128*, 11135 – 11149; c) O. Uzun, Y. Hu, A. Verma, S. Chen, A. Centrone, F. Stellacci, *Chem. Commun.* **2008**, 196 – 198.

[4] a) A. Centrone, E. Penzo, M. Sharma, J. W. Myerson, A. M. Jackson, N. Marzari, F. Stellacci, *Proc. Natl. Acad. Sci. USA* **2008**, *105*, 9886 – 9891; b) J. J. Kuna, K. Voitchovsky, C. Singh, H. Jiang, S. Mwenifumbo, P. K. Ghorai, M. M. Stevens, S. C. Glotzer, F. Stellacci, *Nat. Mater.* **2009**, *8*, 837 – 842.

[5] A. Verma, O. Uzun, Y. Hu, H. S. Han, N. Watson, S. Chen, D. J. Irvine, F. Stellacci, *Nat. Mater.* **2008**, *7*, 588 – 595.

[6] R. P. Carney, J. Y. Kim, H. Qian, R. Jin, H. Mehenni, F. Stellacci, O. M. Bakr, *Nat. Commun.* **2011**, *2*, 335.

[7] C. Leduc, J. Jung, R. P. Carney, F. Stellacci, B. Lounis, *ACS Nano* **2011**, *5*, 2587 – 2592.

[8] A. C. Templeton, D. E. Cliffel, R. W. Murray, *J. Am. Chem. Soc.* **1999**, *121*, 7081 – 7089.

[9] L. M. Demers, C. A. Mirkin, R. C. Mucic, R. A. Reynolds III, R. L. Letsinger, R. Elghanian, G. Viswanadham, *Anal. Chem.* **2000**, *72*, 5535 – 5541.

[10] A. Nykänen, B. Haley, P. D. Zamore, *Cell* **2001**, *107*, 309 – 321.

[11] a) S. Zhou, D. Liang, C. Burger, F. Yeh, B. Chu, *Biomacromolecules* **2004**, *5*, 1256 – 1261; b) S. Sennato, F. Bordi, C. Cametti, M. Diociaiuti, P. Malaspina, *Biochim. Biophys. Acta Biomembr.* **2005**, *1714*, 11 – 24.

[12] a) S. Park, K. Hamad-Schifferli, *ACS Nano* **2010**, *4*, 2555 – 2560; b) D. Kim, J. Kim, M. Park, J. Yeomb, H. Go, S. Kim, M. Han, K. Lee, J. Bae, *Biomaterials* **2011**, *32*, 2593 – 2604; c) P. C. Patel, L. Hao, W. Yeung, C. A. Mirkin, *Mol. Pharm.* **2011**, *8*, 1285 – 1291.

[13] a) T. J. Harris, G. Maltzahn, M. E. Lord, J. Park, A. Agrawal, D. Min, M. J. Sailor, S. N. Bhatia, *Small* **2008**, *4*, 1307 – 1312; b) H. Mok, K. H. Bae, C. Ahn, T. G. Park, *Langmuir* **2009**, *25*, 1645 – 1650.

